International Conference on Applied Energy 2020
Dec. 1 - Dec. 10, 2020, Bangkok / Virtual
Paper ID: 45

Effect of mover assembly mass on the performance of a dual-piston type free piston engine generator

Zhiyuan Zhang, Huihua Feng, Boru Jia*, Zhengxing Zuo

School of Mechanical Engineering, Beijing Institute of Technology, Beijing 100081, China

ABSTRACT

The free piston engine generator (FPEG) is a novel energy conversion device which directly converts chemical energy of fossil fuels into electric energy by linear electric mover's reciprocating linear motion driven by the combustion of combustible fuel-gas mixture. In this research, a validated numerical model was established to investigate the effect of the mover assembly mass on the system operation characteristics, engine performance, heat transfer loss and frictional loss. The results showed that the unique phenomenon of fast expansion and slow compression becomes more obvious as the mover assembly mass increases while the system operating frequency changes slightly. The indicated that the thermal efficiency decreases and the indicated specific fuel consumption increases as the mover assembly mass increases and the maximum indicated power is 3.37 kW when the mover assembly mass is 4.5 kg. The heat transfer loss increases and the friction loss changes slightly as the mover assembly mass increases when the input energy and the effective stroke keep constant. Lower mover assembly mass (lower than 4.0 kg) makes it difficult to achieve high operation compression ratio and higher mover assembly mass and high operation compression ratio would lead to excessive in-cylinder pressure and cause structural damage on the key components.

Keywords: Free piston engine generator, mover assembly mass, operating characteristics, engine performance, heat transfer, thermal efficiency.

NONMENCLATURE

Abbreviations	
FPEG	free piston engine generator

Symbols	
a	shape factor
A	piston area (m^2)
A_f	friction parameters
b	shape factor
B_f	friction parameters
c	load constant ($\mathrm{N}/(m/s)$)
C_d	combustion duration (s)
F_f	mechanical friction force (N)
F_l	gas force from the left cylinder (N)
F_m	linear electric machine force (N)
F_r	gas force from the right cylinder (N)
γ	ratio of heat capacities
h	heat transfer coefficient ($\mathrm{W}/(m^2 \cdot K)$)
H_e	enthalpy of the exhaust air (J)
H_l	enthalpy of the air leak (J)
H_i	enthalpy of the intake air (J)
m	mover assembly mass (kg)
m_{air}	in-cylinder gas mass (kg)
Q_c	heat release from combustion (J)
Q_{ht}	heat transfer loss (J)
Q_{in}	energy input (J)
R	ideal gas constant ($\mathrm{J}/(mol \cdot K)$)
t_s	combustion start time (s)
T_w	cylinder wall temperature (K)
U	internal energy (J)
v	piston velocity (m/s)
V	gas volume (m^3)
x	piston displacement (m)

1. INTRODUCTION

The free piston engine generator (FPEG) is considered as one of the most promising energy conversion device and has attracted the attention from researchers worldwide due to its advantages, e.g. compact structure due to the elimination of the crank mechanism; lower friction loss due to no corresponding side force; higher geometric power ratio and reliability due to a more compact design; multi-fuel suitability due to the variable compression ratio [1-4]. The concept of free piston engine originated in the 1920s and was originally applied to the production of linear compressors [5]. In recent years, with the development of linear motors, free piston engines began to be applied in the field of linear power generation and many researchers have designed FPEG prototypes to study its operation characteristics and control strategies.

The mover assembly contains the mover of the linear electric machine, the pistons connected with the linear electric machine's mover, and the connecting parts such as connecting rods and piston pins. As one of the most important design parameters, the mass of the piston assembly directly affects the operating characteristics of the FPEG and has an important impact on the performance of the free piston engine. Martin Geoertz et al. [6] established a numerical model of a free-piston engine which works on compression ignition two-stroke cycle with direct fuel injection to predict and optimize the design and control parameters. The results showed that the operation frequency increases slightly (by 5%) with the increase of the piston mass and the stroke and the effective compression ratio decreases with a lower piston mass and the same magnetic strength. Q.F. Li et al. [7] at Shanghai Jiaotong University presented the modelling and simulation of a two-stroke spark-ignited free-piston linear alternator and conducted parametric study by a thermodynamic model and a dynamic model. The results showed that the peak pressure increases and the frequency decreases slightly as the mass increases due to the increase of the inertial force and the mass should stay within the 2.1 to 3.5 kg range to make sure the engine runs stably. Nguyen Ba Hung et al. [8] studied a two-stroke spark-ignited free-piston engine which uses a metal spring as a damping device and propane as a fuel by numerical models and simulation which was validated by experimental data. The results showed that by reducing reciprocating mass from m=1.0 kg to m=0.7 kg and keeping the spark timing unchanged, the electric power output increases significantly and the thermal efficiency decreases lightly and the highest electric power output is found at reciprocating mass and spring stiffness of m=0.7 kg and k=14.7 N/mm, respectively.

However, few literature analyses the effect of the mover assembly mass on the performance of a free-piston engine from the perspective of energy breakdown. Simple parametric analysis of mover assembly has no significantly influence on the design and stability control of the FPEG. The purpose of this research is to study the effect of the mover assembly mass on the performance of the FPEG by investigating the differences of the operation characteristics, engine performance, heat transfer loss and friction loss in different mover assembly mass. And provide more accurate suggestions and boundary conditions for the design process and stability control. A detailed numerical model of FPEG which has been validated was established and a prototype has been developed by the authors' group. The operation characteristics and engine performance is analysed with different mover assembly mass and the specific impact is reflected in the way of energy breakdown. Heat transfer loss and friction loss in different mover assembly mass are analysed as well.

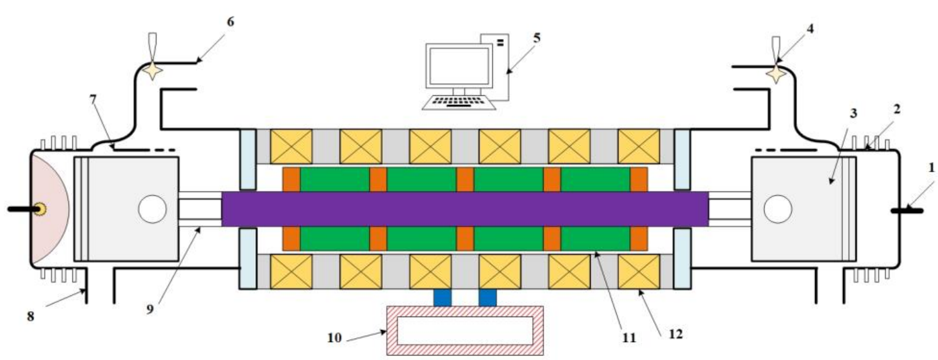

1. Spark plug 2. Cylinder 3. Piston 4. Fuel injector 5. Control system 6. Air-intake tube
7. Scavenging port 8. Exhaust port 9. The connecting rod 10. External load 11. Mover 12. Stator

Fig 1 FPEG schematic configuration

2. PAPER STRUCTURE

2.1 Free piston engine generator configuration

The schematic configuration of a dual-piston dual-cylinder type FPEG is shown in Fig. 1. The linear electric machine is located in the middle of two free-piston engines and the electric machine's mover is connected with the pistons by the connecting rods. The compact structure of this type FPEG makes it have higher power to weight ratio and is favoured by many researchers. A dual-piston dual-cylinder spark-ignited FPEG with a two-stroke thermodynamic cycle prototype was established by the author's group. The intake air and the fuel is mixed in the intake pipe and the mixture gets into the cylinder through the scavenging port and the burned gas is sent out of the cylinder through the exhaust port.

During the operation of the system, the moving part is only the mover assembly which includes the linear electric machine's mover, pistons, connecting rods and piston pins. Therefore, the mass of the mover assembly will have a significantly influence on the system's movement characteristics and the performance of the free-piston engine. The ignition position is adjusted to keep the operation compression ratio constant under different mover assembly mass.

2.2 Numerical modelling and simulation method

The dynamic equation of the mover assembly can be derived from Newton's second law and illustrated in Fig. 2.

$$m\frac{d^2x}{dt^2} = \overrightarrow{F_l} + \overrightarrow{F_r} + \overrightarrow{F_{sr}} + \overrightarrow{F_{sl}} + \overrightarrow{F_m} + \overrightarrow{F_f} \tag{1}$$

where m is the mass of the moving mover assembly (Unit: kg); x is the displacement of the mover (m); F_l is the left cylinder gas force; F_r is the right cylinder gas force (N); F_{sl} and F_{sr} is the gas force from the left scavenging pump and right scavenging pump (N); F_m is the force from the linear electric machine (N); F_f is the friction force (N).

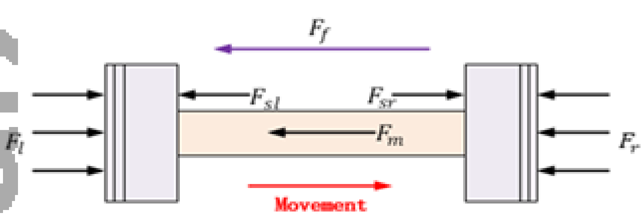

Fig 2 Dynamics of the mover assembly

2.2.1 Numerical modelling and simulation method

According to the first law of thermodynamic, the equation of the in-cylinder gas energy change with time in one cylinder is:

$$\frac{dU}{dt} = -p\frac{dV}{dt} + \left(\frac{dQ_c}{dt} - \frac{dQ_{ht}}{dt}\right) + \sum_i \dot{H}_i - \sum_e \dot{H}_e - \sum_l \dot{H}_l \tag{2}$$

where U is the internal energy of the in-cylinder gas (J); V is the gas volume (m^3); Q_c is the heat release from the combustion process (J); Q_{ht} is the heat transfer loss (J); H_i is the enthalpy of the intake air (J) and H_e is the enthalpy of the exhaust air (J); H_l is the enthalpy of the leaked air (J).

Furthermore, the pressure change equation of the gas in the cylinder can be transformed into:

$$\frac{dp}{dt} = \frac{\gamma - 1}{V}\left(\frac{dQ_c}{dt} - \frac{dQ_{ht}}{dt}\right) - \frac{p\gamma}{m_{air}}\frac{dm_{air}}{dt} - \frac{p\gamma}{V}\frac{dV}{dt} \tag{3}$$

A time based Wiebe function which is modified by the classic Wiebe function to simulate the combustion of FPEG and the heat release in the combustion process can be expressed as [9]:

$$\frac{dQ_c}{dt} = a\frac{b+1}{C_d}\left(\frac{t - t_s^b}{C_d}\right) \cdot exp\left(-a\left(\frac{t - t_s}{C_d}\right)^{b+1}\right)Q_{in} \tag{4}$$

where a and b are shape factors; C_d is the combustion duration (s); t_s is the time the combustion starts (s); Q_{in} is the energy input in one running cycle (J).

In this paper, the Hohenberg heat transfer equation is used to calculate the heat transfer [10]:

$$\dot{Q}_{ht} = hA_{cyl}(T - T_w) \tag{5}$$

$$h = 130V^{-0.06}\left(\frac{p(t)}{10^5}\right)^{0.8} T^{-0.4}\left(v_p + 1.4\right)^{0.8} \tag{6}$$

where $\dot{Q}_{ht}$ is heat flow rate (J/s); h is the heat transfer coefficient ($\mathrm{W}/(m^2 \cdot \mathrm{K})$); A_{cyl} is the area of the cylinder wall in contact with the burned mas (m^2); T is the temperature of the in-cylinder gas (K); T_w is the average cylinder wall temperature (K); v_p is the average piston speed $(\mathrm{m/s})$.

The in-cylinder gas mass changes mainly because of the leakage through the piston rings. A detailed air leakage model is also adopted in the in-cylinder thermodynamics sub-model.

2.2.2 Linear electric generator sub-model

The force of the linear electric generator can be written as:

$$F_m = -cv \tag{7}$$

where c is the load constant of the linear generator ($\mathrm{N}/(m/s)$); v is the velocity of the mover (m/s).

2.2.3 Friction sub-model

An empirical relationship is used to calculate the parameterized friction for the contact between the rings and the cylinder wall:

$$F_{\frac{fring}{liner}} = f\left[-sign(v)\cdot A_f\cdot\sqrt{|v|}\right]\left[1-B_f\cdot\frac{E-\theta_0}{\theta_0}\right]\left[1+K_v\cdot\frac{p(t)}{p_0}\right]\left(\frac{d}{d_0}\right) \tag{8}$$

where f is the overall scaling factor; A_f, B_f and K_v are friction parameters; E is the average temperature of the lubrication at liner (°C); θ_0 is reference temperature (°C); p_0 is reference pressure (bar); d is cylinder diameter (mm) and d_0 is reference cylinder diameter (mm).

Finally, a system level model of a dual-cylinder type FPEG was established in MATLAB/Simulink based on the numerical modelling and is shown in Fig. 3.

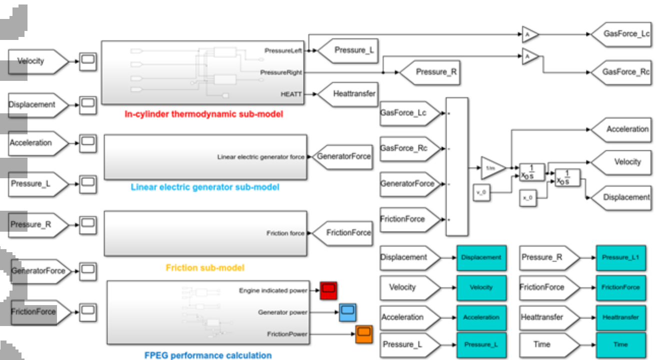

Fig 3 Simulation model in MATLAB/Simulink

2.2.2 Model validation

The numerical model has been validated with the experimental data from the prototype both in the cold start-up process and the stable generating process. For more details on the numerical modelling and validation results, please refer the previous publications published the authors' group [11-13].

2.3 Results

2.3.1 FPEG piston operating characteristics in different mover assembly mass

Fig. 4 shows the piston velocity-displacement curves of the FPEG in different mover assembly mass when the input energy and the compression ratio keep constant. The results show the unique operating characteristics of the FPEG: fast expansion, slow compression. And this unique phenomenon becomes more obvious as the mover assembly mass decreases. Due to the difference in acceleration caused by the difference of mover assembly mass, the piston velocity is lower as the mover assembly mass decreases near the dead centre. The acceleration-velocity diagram is shown in Fig. 5. The maximum acceleration increases first and then decrease as the mover assembly mass increases. In acceleration increasing stage, the acceleration increases with the increase of the mover assembly mass, and after the acceleration reaches the maximum, as the mover assembly mass increases, the acceleration becomes smaller. Therefore, the acceleration change is affected by the in-cylinder pressure and the mover assembly mass and the change of ignition position is also the important influencing factor of in-cylinder pressure.

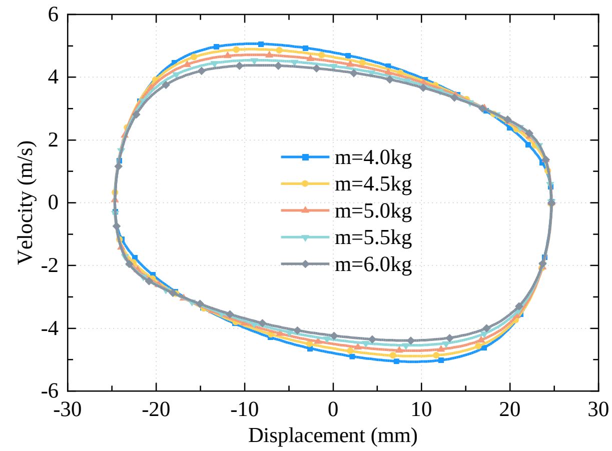

Fig 4 FPEG velocity-displacement diagram in different mover assembly mass

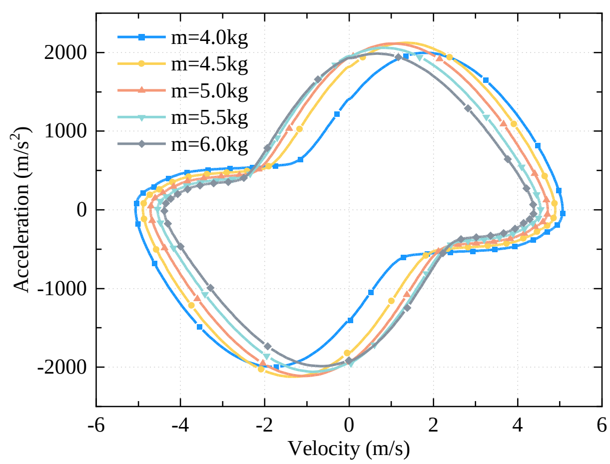

Fig 5 FPEG acceleration-velocity diagram in different mover assembly mass

Fig. 6 shows the operation frequency and the piston average velocity change in different mover assembly mass. The results show that the mover assembly mass has little effect on operation frequency and the maximum operation frequency is 33.7 Hz when the mover assembly mass is 4.5 kg.

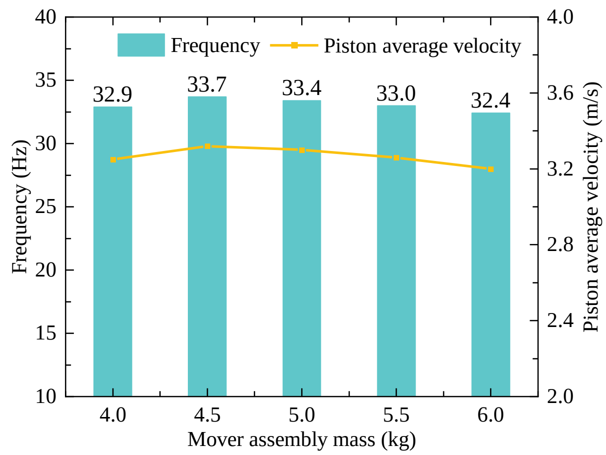

Fig 6 FPEG operation frequency and piston average velocity in different mover assembly mass

2.3.1 FPEG engine performance in different S/B ratios

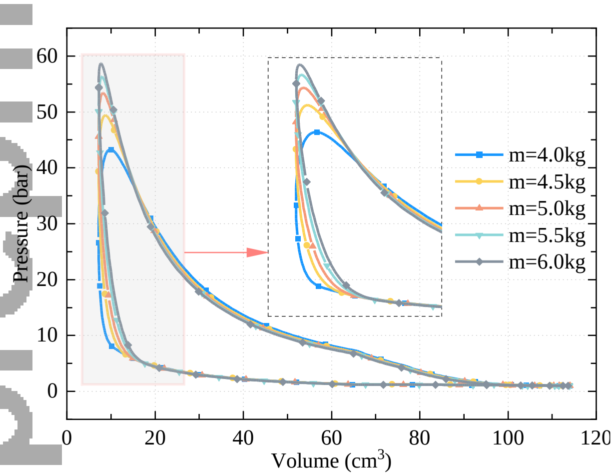

Fig 7 FPEG in-cylinder pressure in different mover assembly mass

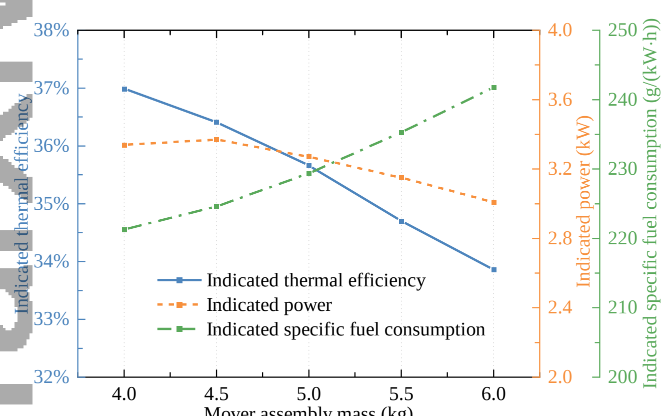

Fig 8 FPEG engine performance in different mover assembly mass

Fig. 7 shows the change of in-cylinder pressure in indifferent mover assembly mass when the operation compression ratio keeps constant. The maximum in-cylinder pressure increases as the mover assembly mass increases. The combustion cycle is closer to the isometric cycle as the mover assembly mass decreases. Therefore, as can be seen from Fig. 8, the indicated thermal efficiency decreases with the increasing of the mover assembly mass. The change of the indicated specific fuel consumption is opposite and the maximum indicated power is 3.37 kW when the mover assembly mass is 4.5 kg.

2.3.1 FPEG energy breakdown in different mover assembly mass

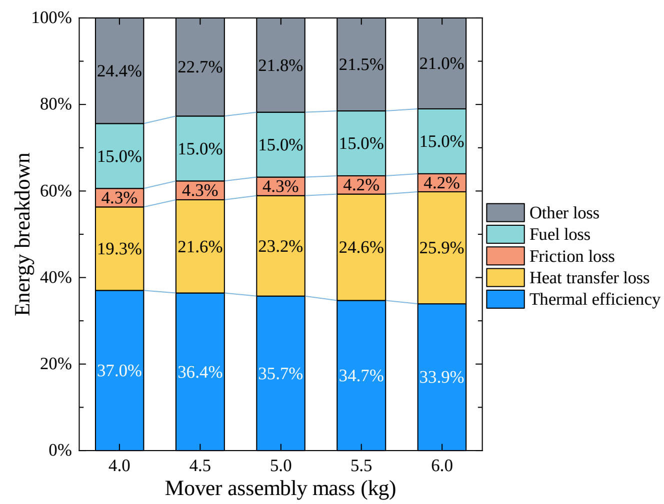

Fig 9 FPEG energy breakdown in different mover assembly mass

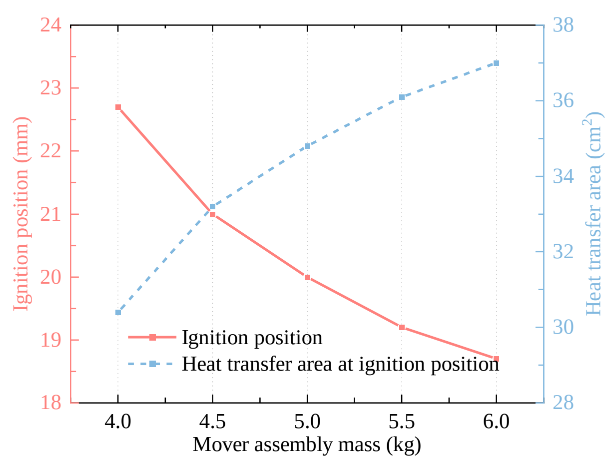

Fig 10 FPEG heat transfer area at ignition position in different mover assembly mass

Fig. 9 shows the energy breakdown of the FPEG in different mover assembly mass when the input energy keeps constant and the fuel loss caused by the scavenging and incomplete combustion is set to 15%.

The difference in friction loss is slight because the operation compression is same which makes that the effective stroke keeps same in different mover assembly mass. The heat transfer loss decreases as the mover assembly mass increases due to the increase of the heat transfer area at the ignition position which can be seen from Fig. 10.

2.4 Discussion

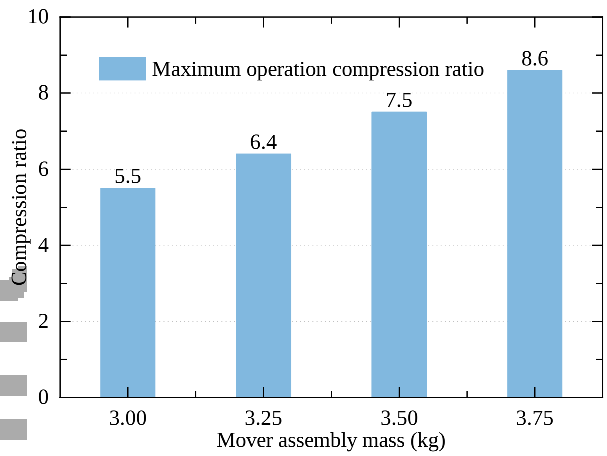

Fig 11 The maximum operation compression ratio when the mover assembly mass is lower than 4.0 kg

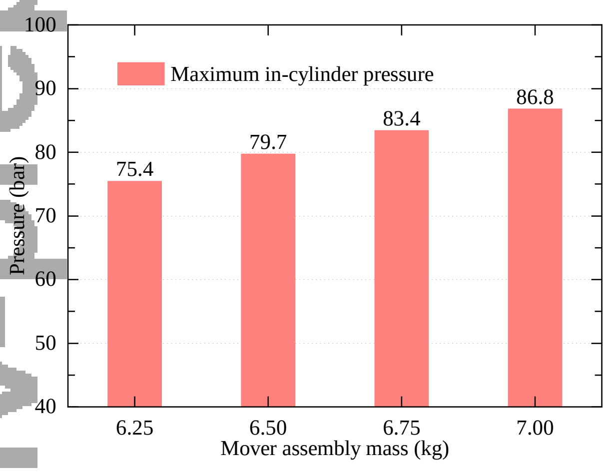

Fig 12 The maximum operation compression ratio and in-cylinder pressure when the mover assembly mass is higher than 6.0kg

When the mover assembly mass is lower than 4.0 kg, the maximum operation compression ratio is shown in Fig. 11. The results show that low mover assembly mass will limit the system's operating compression ratio and even make the free-piston engine misfire. The limitation of the compression ratio also limits the performance of the free-piston engine. However, when the mover assembly mass increases, the indicated thermal efficiency decreases and the indicated specific fuel consumption increases as can be seen from Fig. 8. And if the mover assembly mass is higher than 6.0 kg, although there is no limit to the compression ratio, an excessively high operation compression ratio will make the in-cylinder pressure too high as shown in Fig. 12. Therefore, in the design stage, the mass of the mover assembly needs to be selected based on the performance and structural factors of the free-piston engine.

2.5 Conclusions

In this research, the effect of the mover assembly mass on the performance of the FPEG in the stable generating process was investigated. A detailed numerical model was established in MATLAB/Simulink and the accuracy of the model was validated by the experimental data in the authors' previous research.

The simulation results show that the unique phenomenon of fast expansion and slow compression becomes more obvious as the mover assembly mass decreases and the operation frequency and the average piston velocity change slightly as the mover assembly mass changes and the maximum operation frequency is 33.7Hz when the mover assembly mass is 4.5 kg.

The indicated thermal efficiency decreases and the indicated specific fuel consumption increases as the mover assembly mass increases and the maximum indicated power is 3.37 kW when the mover assembly mass is 4.5 kg. The friction loss changes slightly due to the fixed effective stroke and the heat transfer loss increases as the mover assembly mass increases because the ignition position is further forward to keep the operation compression constant.

When the mover assembly mass is lower than 4.0 kg, the maximum operation compression ratio is lower than 9, and if the mover assembly mass is higher than 6.0 kg, the in-cylinder pressure is too high and there may be structural damage to key components when the FPEG is operated in high compression ratio.

ACKNOWLEDGEMENT

This project is supported by the National Natural Science Foundation of China (project number: 51675043), and Beijing Institute of Technology Research Fund Program for Young Scholars. The authors would like to thank the sponsors.

REFERENCE

[1] Mikalsen R, Roskilly AP. A review of free-piston engine history and applications. Applied Thermal Engineering. 2007;27:2339-52.

[2] Hung NB, Lim O. A review of free-piston linear engines. Applied Energy. 2016;178:78-97.

[3] Hanipah MR, Mikalsen R, Roskilly AP. Recent commercial free-piston engine developments for automotive applications. Applied Thermal Engineering. 2015;75:493-503.
[4] Jia B, Mikalsen R, Smallbone A, Roskilly AP. A study and comparison of frictional losses in free-piston engine and crankshaft engines. Applied Thermal Engineering. 2018;140:217-24.
[5] Pateras PR. Motor-compressor apparatus. US; 1928.
[6] Goertz M, Peng L. Free Piston Engine Its Application and Optimization. SAE International; 2000.
[7] Li QF, Xiao J, Huang Z. Parametric study of a free piston linear alternator. International Journal of Automotive Technology. 2010;11:111-7.
[8] Hung NB, Lim O. A study of a two-stroke free piston linear engine using numerical analysis. Journal of Mechanical Science Technology. 2014;28:1545-57.
[9] Kim J, Bae C, Kim G. Simulation on the effect of the combustion parameters on the piston dynamics and engine performance using the Wiebe function in a free piston engine. Applied Energy. 2013;107:446-55.
[10] Hohenberg GF. Advanced Approaches for Heat Transfer Calculations. SAE Transactions. 1979;88:2788-806.
[11] Jia B, Zuo Z, Feng H, Tian G, Roskilly AP. Investigation of the Starting Process of Free-piston Engine Generator by Mechanical Resonance. Energy Procedia. 2014;61:572-7.
[12] Jia B, Tian G, Feng H, Zuo Z, Roskilly AP. An experimental investigation into the starting process of free-piston engine generator. Applied Energy. 2015;157:798-804.
[13] Jia B, Smallbone A, Zuo Z, Feng H, Roskilly AP. Design and simulation of a two- or four-stroke free-piston engine generator for range extender applications. Energy Conversion and Management. 2016;111:289-98.

